Impact of manufacturing changes on Zr alloy in-pile performance

Authors

Peter Rudling
ANT International, Skultuna, Sweden

Ron Adamson
Zircology Plus, Fremont, Pleasanton, CA, USA

Brian Cox
University of Toronto, Ontario, Canada

Friedrich Garzarolli
Fürth, Germany

Alfred Strasser
Aquarius Services, Sleepy Hollow, NY, USA

Antonina Nikulina
A. A. Bochvar All-Russian Research Institute of Inorganic Materials, Moscow, Russia

Slava Shishov
A. A. Bochvar All-Russian Research Institute of Inorganic Materials, Moscow, Russia

Reviewed by

Charles Patterson
Clovis, CA, USA

A.N.T. INTERNATIONAL®

Advanced Nuclear Technology International
Krongjutarvägen 2C, SE-730 50 Skultuna
Sweden

info@antinternational.com
www.antinternational.com

Disclaimer

The information presented in this report has been compiled and analysed by Advanced Nuclear Technology International Europe AB (ANT International®) and its subcontractors. ANT International has exercised due diligence in this work, but does not warrant the accuracy or completeness of the information. ANT International does not assume any responsibility for any consequences as a result of the use of the information for any party, except a warranty for reasonable technical skill, which is limited to the amount paid for this assignment by each ZIRAT/IZNA programme member.

Contents

1 Introduction

To ensure safe operation of nuclear fuel, certain performance criteria must be met both during normal operation, anticipated operational occurrences and during postulated accidents. Zr Alloy material properties impact some of the most important performance criteria such as:

- Pellet Cladding Interaction (PCI) Pellet Cladding Mechanical Interaction (PCMI) corrosion and hydriding properties that, in turn, are dependent upon:
  - Chemical composition.
  - Crystallographic texture and cladding microstructure.
  - Clad strength/ductility/fracture toughness.
- Re-opening of the pellet-cladding gap, lift-off, which is partly related to the fuel clad creep properties.
- Excessive dimensional changes (resulting in e.g. excessive Fuel Assembly (FA) bowing) of fuel components that are a function of creep (including oxide induced and residual stress relaxation creep), irradiation growth, and hydrogen pickup in the components.
- Loss of Coolant Accident (LOCA) performance that is related to hydrogen pickup both during the base irradiation, before the LOCA event, as well as during the high temperature LOCA oxidation.

The Zr-alloy properties are a function the reactor environment (fast neutron flux, temperature, water chemistry, etc.) and the Zr-alloy microstructure. The microstructure is a function of material chemistry and the manufacturing process. A better knowledge of the impact of manufacturing changes on the Zr alloy microstructures and in-pile material properties can lead to improved capabilities to respond to current fuel performance issues and to ensure that any changes in the current manufacturing processes of the Zr alloys will not impair the fuel safety performance criteria. The overall objective of this Special Topic Report (STR) is to provide this knowledge.

The Report structure is as follows:

- Section 2 describes briefly the various Zr alloys that are being commercially used in the nuclear industry as well as provides an outline of the Zr alloy manufacturing industry.
- Section 3 goes through the Zr alloy manufacturing process steps from Zr sponge manufacturing to final tube production and, for each process step, discusses their impact on in-pile performance. More information on this topic is given in the Fuel Fabrication Process Handbook (FFPH) [Strasser & Rudling 2004], Fuel Material Technology Report (FMTR) Vol. 1 [Cox et al 2006], in FMTR Vol. 2 [Rudling et al. 2007] and the following ZIRconium Alloy Technology (ZIRAT)/Information on Zirconium Alloys (IZNA) STRs:
  - **Corrosion & Hydriding Topics**
    - Corrosion of Zirconium Alloys, ZIRAT7/IZNA2, [Adamson et al 2002/2003].
    - Corrosion of Zr-Nb Alloys in PWRs, ZIRAT9/IZNA4, [Cox et al 2004/2005].
    - Corrosion Mechanisms, ZIRAT12/IZNA7, [Adamson et al 2007/2008a].

- **Mechanical Property Topics**
  - Mechanical Properties of Zirconium Alloys, ZIRAT6/IZNA1, [Adamson & Rudling 2001/2002].
  - Hydriding Mechanisms and Impact on Fuel Performance, ZIRAT5/IZNA1, [Cox & Rudling 2000].
  - Pellet Cladding Interaction and Pellet Cladding Mechanical Interaction, ZIRAT11/IZNA6, [Adamson et al 2006/2007a].
- **Manufacturing Topics**
  - Manufacturing of Zirconium Alloy Materials, ZIRAT5/IZNA1, [Rudling & Adamson 2000].
  - Manufacturing of Zr-Nb alloys, ZIRAT11/IZNA6, [Nikulina et al 2006/2007].
  - Welding of Zirconium Alloys, ZIRAT12/IZNA7, [Rudling et al 2007/2008].
- **Dimensional Changes Topics**
  - Dimensional Instability, ZIRAT7/IZNA2, [Adamson & Rudling 2002/2003].
  - Structural Behaviour of Fuel Components, ZIRAT10/IZNA5, [Cox et al 2005/2006].
- **Other Topics**
  - Impact of Irradiation on Material Performance, ZIRAT10/IZNA5, [Adamson & Cox 2005/2006].
  - The Effect of Hydrogen on Zirconium Alloy Properties, ZIRAT13/IZNA8, Vol. I, [Strasser et al 2008/2009a].
  - The Effect of Hydrogen on Zirconium Alloy Performance, ZIRAT13/IZNA8, Vol II, [Strasser et al 2008/2009b].

- Appendix A gives a summary of texture development and Appendix B more detailed information about the development of the various Annealing Parameters being used.

2 Application of Zr components in the FA and industry structure

Zirconium alloys are used as much as possible in the FA as structural materials due to their properties as follows:

- Low thermal neutron cross section
- Adequate mechanical properties
- Adequate corrosion properties
- Adequate high temperature oxidation properties

Since pure Zr has poor (at best unpredictable) water/steam corrosion resistance, it needs to be alloyed. (Table 2-1) list the currently used Zr-materials.

Table 2-1: Commercial zirconium base materials currently used for zirconium alloy fuel components in Pressurised Water Reactor (PWRs), Boiling Water Reactor (BWRs), Canadian Deuterium Uranium (CANDU), Voda Voda Energo Reactor (VVER), Reaktor Bolshoi Mozhnosti Kanalov (in English Large Boiling Water Channel type reactor) (RBMK).

Alloy	Sn %	Nb %	Fe %	Cr %	Ni %	O %	Fuel Vendor
BWRs							
Zircaloy-2 (SRA[1)]/RXA[2)])[1]	1.2-1.7	-	0.07-0.2	0.05-0.15	0.03-0.08	0.1-0.14	All fuel vendors
Zr-Liner[2]							
Sponge	-	-	0.015-0.06	-	-	0.05-0.1	Only used in Japan and Russia
ZrSn	0.25	-	0.03-0.06	-	-	0.05-0.1	Westinghouse
ZrFe	-	-	0.4	-	-	0.05-0.1	AREVA
ZrFe	-	-	0.10	-	-	0.05-0.1	GNF[3)] P8[3]
PWRs							
Zircaloy-4 (SRA)	1.2-1.7	-	0.18-0.24	0.07-0.13	-	0.1-0.14	Only used in Japan and France
ZIRLO (SRA)	1	1	0.1	-	-	0.12	Westinghouse
Optimized ZIRLO (SRA/pRXA[4)])	0.7	1	0.1	-	-	0.12	Westinghouse
M5 (RXA)	-	0.8-1.2	0.015-0.06	-	-	0.09-0.12	AREVA
HPA-4[5)] (SRA/RXA)	0.6	-	Fe+V	-	-	0.12	AREVA
NDA[6)] (SRA)	1	0.1	0.3	0.2		0.12	NFI[7)]
MDA[8)] (SRA)	0.8	0.5	0.2	0.1		0.12	MHI[9)]
Duplex[4]							
ELS[10)][5]	0.5/0.8	-	0.3/0.5	0.2	-	0.12	AREVA
D4	0.5	-	0.7	-	0.12		AREVA
3b[6]	<0.8	-		<0.6			Westinghouse
3b+[7]	<1.0	-		<0.6			Westinghouse
D4[8]	<0.8	-		<0.6			Westinghouse
VVER, RBMK							
E-110 (RXA)	-	0.9-1.1	0.014	<0.003	0.0035	0.05-0.07	Fuel cladding
Alloy E125 (SRA)	-	2.5	-	-	-	0.06	Pressure tube in RBMK
CANDU							
Zircaloy-4 (SRA)	1.2-1.7	-	0.18-0.24	0.07-0.13	-	0.1-0.14	Fuel cladding
Zr2.5Nb (SRA)	-	2.4-2.8	<0.15	-	-	0.09-0.13	Pressure tube

[1)] Stress Relieved Annealed [2)] Recrystallised Annealed [3)] Global Nuclear Fuel [4)] Partially Recrystallised Condition [5)] High Performance Alloy [6)] New Developed Alloy [7)] Nuclear Fuel Industries [8)] Mitsubishi Developed Alloy [9)] Mitsubishi Heavy Industries [10)] Extra-Low Sn

[1] All but one of the BWR fuel vendor use RXA, fuel cladding. The exception uses SRA, fuel cladding.
[2] In all BWR cladding with liners, about 90 % of the thickness-the outer part of the tube consists of Zry-2.
[3] Starting with Process 8 (P8), GNF adopted a liner that contains somewhat higher Fe content than that the earlier liners (P7 and earlier).
[4] All DUPLEX claddings consist of an outer corrosion resistant layer with a thickness < 100 microns and the rest of the thickness is Zry-4 to provide the mechanical strength.
[5] All AREVA duplex claddings contains Zry-4 with 1.5 wt%Sn
[6] Zry-4 with 1.3 wt %Sn
[7] Zry-4 with 1.5 %Sn
[8] Zry-4 with 1.5%Sn

(Figure 2-1) summarises the structure of the industry. As listed in (Table 2-2), Zr-sponge is being manufactured by Companie Europen Ziconium Ugine Sandvik (CEZUS) in France (within the AREVA corporation), ATI Wah Chang, (independent) and Western Zirconium (WZ) (within the Westinghouse corporation) in USA. WZ also delivers tube shells, sheet, strip and bar stock to Global Nuclear Fuels (GNF) Some limited amounts of Zr-sponge are in addition being produced in India and Argentina. All the zirconium used in VVER fuel elements is produced in a plant at Glazov in the Russian Federation. This plant is unique in the world since it does not use the Kroll process but an electrolytic process to produce the Zr raw material (however, they are now planning to change this process to the Kroll process).

CEZUS also manufacture strip/sheet and tubes for AREVA, see (Table 2-3). AREVA cladding is also being produced at a facility in Duisburg, Germany.

AB Sandvik Steel (ABSS) in Sweden and Sandvik Special Metal (SSM) in USA are independent manufacturers (i.e. not tied to a specific fuel vendor) and produces tubes from tube shells or TREX purchased from either CEZUS or ATI Wah Chang.

Carpenter in USA manufactures fuel outer channels, primarily for AREVA.

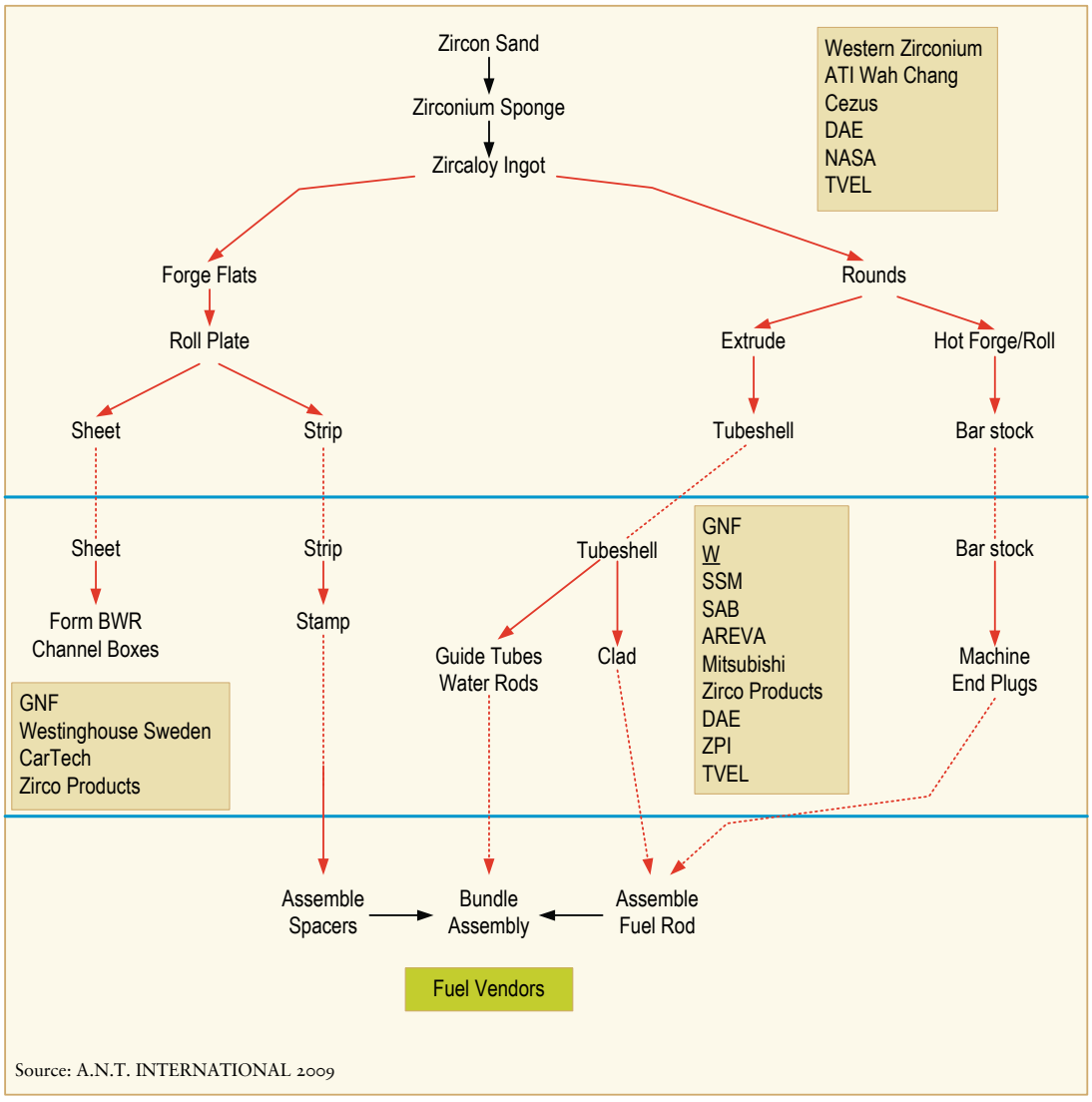

Figure 2-1: Zircaloy production outline.

Table 2-2: Zr metal production, [World Nuclear Industry Handbook 2008].

Product	Location	Company	Capacity per year (tons)	Process used
Zr Sponge from Zircon sands	Jarrie, France	AREVA[9]	2200	Chlorination – Kroll reduction
Zr sponge, Crystal bar from Zircon sands	Hyderabad, India	DAE	210	Not available
Zr sponge, Crystal bar from Zircon sand	Albany, Oregon, USA	ATI Wah Chang[10]	2000	Kroll reduction
Zr-metal from Zircon sand	WZ Plant, USA	Westinghouse	3 000 000	Not available
Zr sponge, Crystal bar from Zircon sand	Glazov, Russia	TVEL	Not available	Electrolytic process
Zr sponge, Crystal bar from Zircon sand	Ezeiza (ZMP), Argentina	NASA	Not available	Not available

[9] Previously CEZUS
[10] Previously Teledyne Wah Chang

Table 2-3: Tubing, bars stock, flat product and fuel outer channel vendors, [World Nuclear Industry Handbook 2008].

Product	Location	Company	Capacity per year (tons)	Process used
Tubing				
TREX from Zr sponge	Ugine, France	AREVA[11]	5000	Melting, forging, extrusion and swaging
Tubes from TREX	Montreuil Juigne, France	AREVA [12]	1200	Pilgering
Cladding and guide tubes from Zr tubing	Paimboeuf, France	AREVA [13]	5000 km/y	Pilgering
Tubes	Nagahama, Japan	AREVA [14]	300	Not available
Zr tubing from Zr metal	Duisburg, Germany	AREVA	2 200 km/y	Not available
Tubing from Zr sponge	Hyderabad, India	DAE	80	Not available
Zr tubing (from Zr metal)	Amagasaki, Japan	Zirco Products[15]	350	Not available
Zr tubing from Zr metal	Arnprior, Canada	GNF	1600 km	Not available
Zr tubing from Zr metal	Cobourg, Canada	ZPI	760	Not available
TREX from Zr-sponge	Albany, Oregon, USA	ATI Wah Chang[16]	Not available	Not available
Zr tubing from Zr sponge[17]	Wilmington, USA	GNF	Not available	Not available
Zr tubing from Zr alloy	Specialty Metals USA	Westinghouse	13 000 000 ft/y	Not available
Zr tubing from Zr metal	Kennewick, USA	SSM	2200	Not available
Zr tubing from Zr metal	Allens Park, USA	Nikko	500	Not available
Zr tubing	Chepetsky Plant, Glazov, Udmurtia	TVEL	2000 km/y (1992)[18]	Not available
Zr tubing Zr from sponge	Sandviken, Sweden	Sandvik Steel	1200	Not available
Bar stock				
Ingots/barstock/TREX	Ugine, France	AREVA [19]	5000	Melting, forging, extrusion and swaging
Flat products				
Strips/sheets from slabs	Rugle, France	AREVA [20]	450	Hot and cold rolling
Strips/sheets from slabs	Albany, Oregon, USA	ATI Wah Chang[21]	Not available	Not available
BWR Fuel Outer Channels				
BWR Fuel Outer Channels[22]	USA	Carpenter	Not available	Not available

[11] Previously CEZUS
[12] Previously CEZUS
[13] Previously Zircotube
[14] Previously Zircotube
[15] Previously Sumitomo
[16] Previously Teledyne Wah Chang
[17] In the case of GNF, as an example, the feed material is sponge in the form of Zry-2+Zr metal tube shells.
[18] IAEA Report No 379: "Design and Performance of VVER Fuel", IAEA, Vienna, 1996.
[19] Previously CEZUS
[20] Previously CEZUS
[21] Previously Teledyne Wah Chang
[22] GNF also manufactures channels at its facility in Wilmington, NC using strip from (primarily) from WZ.

3 Relationship between fabrication, microstructure and performance

3.1 Introduction

This section gives an overview on how the tubular manufacturing processes impacts the microstructure and in turn the fuel performance, (Figure 3-1).

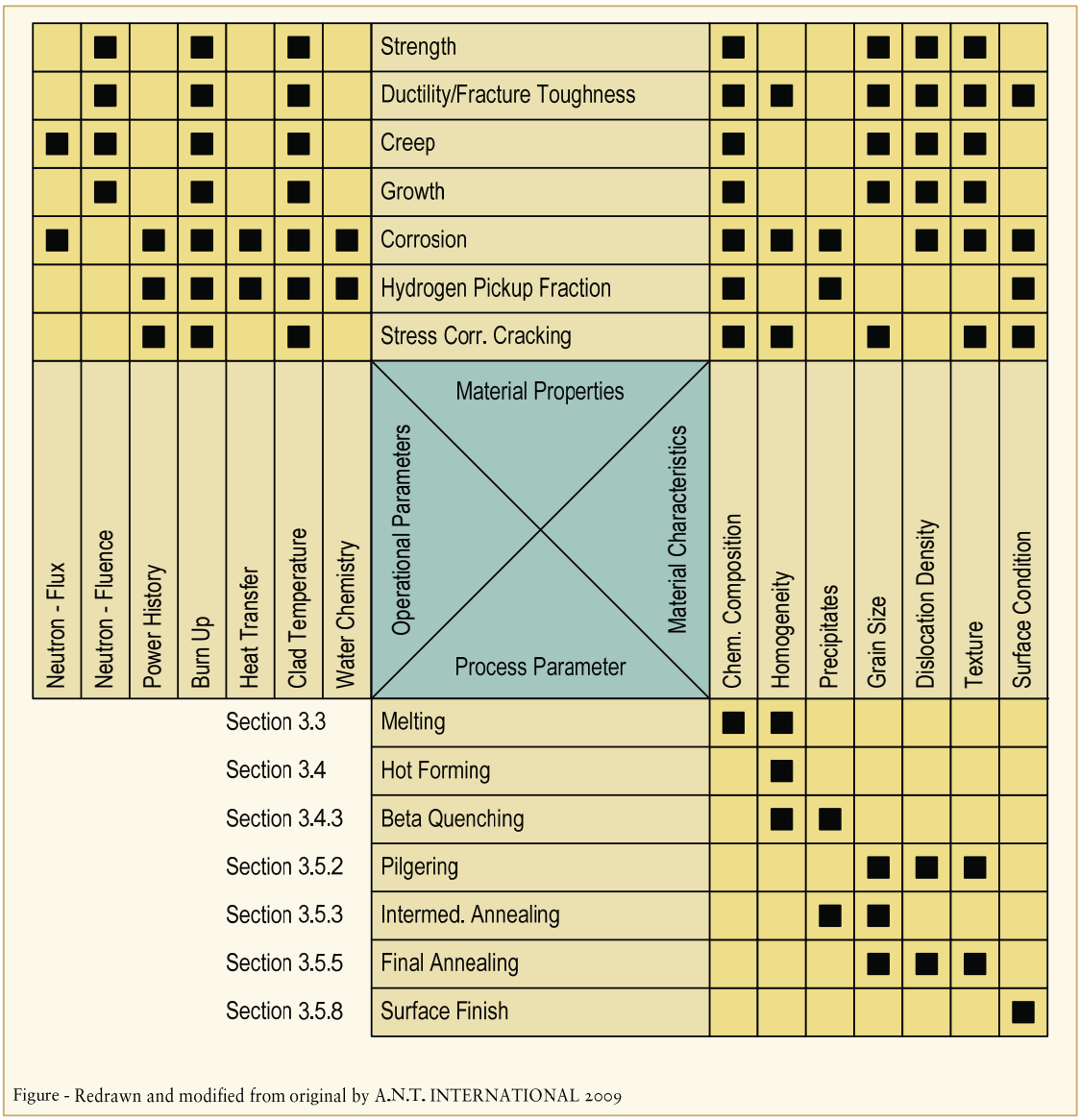

Figure 3-1: The relation between material properties, operation parameters, material characteristics and manufacturing processes. Hydrogen pickup fraction is a measure of the fraction of the hydrogen produced in the corrosion reaction between zirconium alloy and water which is pickup up by the zirconium alloy material. The section number relates to sections in this report where more information is given for each manufacturing step. The figure is a revision of the one used by [Strasser et al 1994].

As an example of the impact of the parameters mentioned above on fuel performance we can consider PCI performance of a fuel rod that is related to:

- The stress corrosion cracking properties (material properties) of the fuel clad inner surface that in turn is a function of parameters such as:
  - Material characteristics (microstructure) that are a function of:
    - Chemical composition of the clad inner surface.
    - Homogeneity
    - Grain size of the fuel cladding
    - Texture
    - Clad inner surface condition
- Operational parameters (reactor environment):
  - Power History (ramp rate and ramp terminal level (impacts the clad tensile stress level during the ramp).
  - Burnup which will impact:
    - The concentration of stress corrosion agents formed in the fuel (Iodine, Cesium and Cadmium).
    - Pellet/Cladding gap due to pellet swelling and clad creep down.

3.2 Zirconium metal production

3.2.1 Introduction

The Swedish chemist Berzelius succeeded in 1824 to produce impure zirconium powder by reduction of potassium zirconium fluoride with sodium. In 1865 Troost was able to produce impure metal by reducing gaseous zirconium tetrachloride with magnesium. It was not until in 1925 that Van Arkel, DeBoar and Fast succeed in developing the first practical method for producing ductile zirconium. Their method was based upon an iodine process in which zirconium iodide decomposes on a hot filament. However, this method is very expensive and it would not be possible to produce large quantities of zirconium with this method. This material is called “crystal bar or iodide Zr”.

In the second part of the 1940’s, Dr. Kroll succeeded in developing a more economical process at Albany, Oregon, for production of ductile zirconium by reduction of zirconium tetrachloride with molten magnesium in an inert atmosphere. This material is called “sponge Zr”.

A third method was used in the former Soviet Union to electrolytically produce Zr metal.

All fuel vendors are using Zr metal (sponge Zirconium) by the Kroll process except for the Russians that have been using Zr metal from a mixture of Zr produced through the Van Arkel and the electrolytic processes. The Russians are however going to shift to Zr metal from the Kroll Process.

Nearly all the zirconium metal is extracted from zircon sand, Zr-Hf SiO_4, occurring in beach sand all over the world. The zirconium to hafnium ratio in zircon is about 50/1 but since Hf has a very large thermal neutron cross section, it is crucial that as much Hf as possible is separated from zirconium during the manufacturing process.

The alloy homogeneity and chemical impurity concentrations of the final products is mainly established in the very first steps, starting from the zirconium sand, i.e. hafnium separation, ZrO_2 reduction, scrap recycling and ingot melting. Only the gas contents can be influenced also in later processes.

The three commercial processes to which are used to produce Zr metal are described in the following sub-sections; i.e., the Kroll process (used by most Zr manufacturers), the Van Arkel process and the electrolytic process.

3.2.2 Process

3.2.2.1 Kroll process

The first step is to convert zircon into $ZrCl_4$, through a carbo-chlorination process performed in a fluidised bed at 1200 °C, (Figure 3-2).

After the Zr/Hf separation process, Zr metal is obtained by Zr-reduction in which gaseous $ZrCl_4$ is reduced by liquid magnesium at 850 °C in an oxygen-free environment (Kroll process). Any Mg remnants are subsequently removed from the sponge cake by distillation at 1000 °C. The sponge cake is then fractured and the pieces are carefully inspected and contaminated pieces showing up as discoloration are discarded. *The sponge impurity levels of Cl and Mg are determined by this process step.*

The appropriate American Society for Testing and Materials (ASTM) specification for nuclear grade zirconium sponge is B349. Typical sponge chemical content is shown in (Table 3-1).

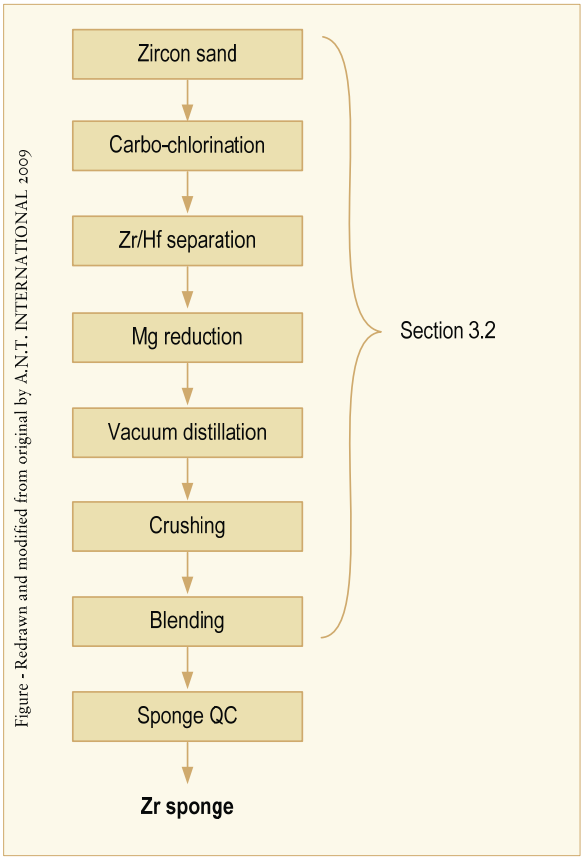

Figure 3-2: General process flow diagram for Zr sponge fabrication. The section number relates to sections in this report where more information is given for each manufacturing step.

Table 3-1: Typical chemical composition of Zr produced by the Kroll process.

Element	Impurity, ppm (Zr balance)
Fe	200-500
Cr	65
Al	25
Ti	25
Si	40
Cu	5
W	25
Hf	75
Mg	--
O	1100
C	110
N	45

3.2.2.2 Van Arkel process

High purity Zr can be obtained by the Van Arkel process which consists of reaction of Zr with iodine at moderate temperature, gaseous phase transport as ZrI_4 and decomposition of the iodide at high temperature on an electrically heated filament, (Table 3-2). This process is considerably more expensive than either the electrolytic or the Kroll process but produces zirconium of high purity, as can be seen by comparing (Table 3-1) and (Table 3-2).

Table 3-2: Typical chemical composition of Zr produced by the Van Arkel Process.

Element	Zr-X-Bar[1)] Impurities (ppm)
Fe	6
Cr	3
Al	2
Ti	<0.1
Si	0.2
Cu	0.1
W	<0.1
Hf	26
Mg	<0.1
O	70
C	25
N	<0.10
[1)] Analyzed by GDMS	

3.2.2.3 Electrolytic process

All the zirconium used in VVER fuel elements is produced in a plant at Glazov in the Russian Federation, [International Atomic Energy Agency (IAEA) No. 379, 1996]. This plant is unique in the world in using neither the Kroll process nor the Van Arkel process, but an electrolytic process. However, the Russians are going to change to the more inexpensive Kroll Process, see Section 3.2.2.1

Before the electrolytic extraction of Zr, the concentration of Hf of the feed material is reduced by fractional distillation of zirconium silicate.

The sand ($ZrSiO_4$) is first reacted with K_2SiF_6 to produce K_2ZrF_6 in a separate operation. In the extraction process, the electrolyte used is K_2ZrF_6 in KCl. The process operates in closed gas tight electrolytic cells at high temperature under an inert atmosphere. The current used is in the range 10 000 to 20 000 A, and the cell is water cooled externally so that the cell surfaces are covered with a layer of solidified electrolyte which avoids the pick-up of impurities. K_2ZrF_6 is consumed as Zr is deposited on the cathode. Zirconium is produced as a powder, and after pre-treatment it is mixed with pure scrap metal that has been purified by the Van Arkel process and the alloying addition, in most cases only Nb, either 1% or 2.5%.

The chemical content of Zr manufactured by the electrolytic process has lower impurity concentrations compared to that of Zr manufactured by the Kroll process but higher than that produced by the Van Arkel process.

3.2.3 Impact of Zr source material on in-pile performance

3.2.3.1 LOCA oxidation

Results from a large research program, which was presented by [Yegorova et al 2004] revealed that the high temperature oxidation rate (such as during a LOCA) of E110 cladding manufactured from the sponge Zr is comparable to that of M5 and is much less than that for the E110 cladding manufactured from iodide/electrolytic Zr (that is the normal base material used for E110 and E635 materials), (Figure 3-3) and (Figure 3-4). The greater protectiveness of the oxide formed on the E110 manufactured from Zr sponge material also reduces the hydrogen pickup fraction, (Figure 3-5).

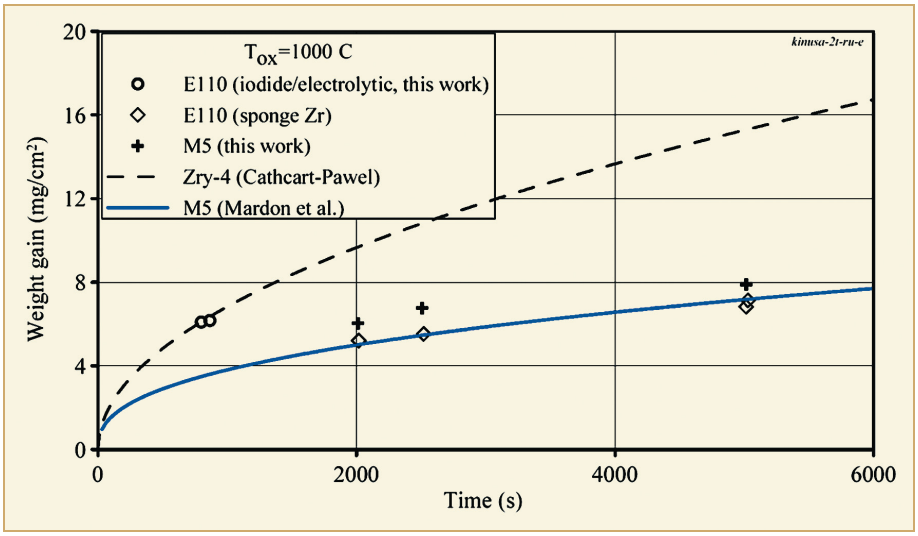

Figure 3-3: The predicted oxidation kinetics of zirconium-niobium alloys manufactured from the sponge Zr at 1000 °C, [Yegorova et al 2004].

E110 (iodide/electrolytic Zr) ECR=7.7%	t_{ef}=865 s	
E110 (sponge Zr) ECR=8.9% (H_2→11 ppm)	t_{ef}=5028 s	

Figure 3-4: Surface appearance of two types of E110 claddings after the oxidation at 1000 °C, [Yegorova et al 2004].

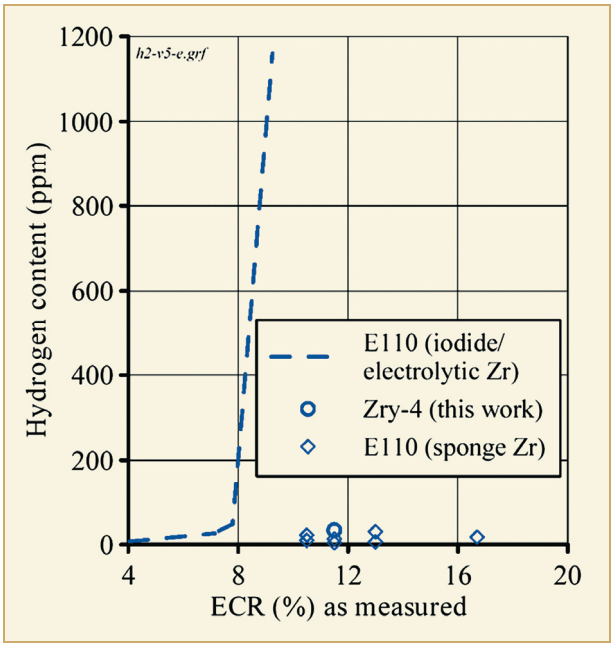

Figure 3-5: Hydrogen pickup of different E110 materials oxidised at 1100 C, [Yegorova et al 2004].

Thus, it appears that the main reason for the difference in LOCA behaviour between the Russian alloys E110/E635 and Zry-4/ZIRLO/M5 is related to the differences in the early manufacturing of these two different groups of materials. E110/E635 alloys are manufactured from iodide/electrolytic Zr while Zry-4/ZIRconium Low Oxidation (ZIRLO)/M5 is manufactured from Zr sponge resulting in small differences in impurity levels. [Chung 2004] suggests that the impurities Ca, Mg and Al that are found in larger concentrations in sponge Zr than in the Russian Zr base material improves protectiveness of the formed oxide during the LOCA event, while F that occurs in much higher concentrations in the Russian material deteriorates the oxide protectiveness. *However, the impurities responsible for the improvement in the oxidation and hydriding resistance of the Kroll manufactured Zr source metal have not yet been clearly identified. Increased hydrogen pickup of the fuel cladding during the high temperature LOCA oxidation will increase the embrittlement of the cladding during quenching from the LOCA oxidation temperature as well as during post-LOCA events.*

More information may be obtained e.g. in Section 3.2.3. in ZIRAT9/IZNA4 STR on LOCA and RIA.

3.2.3.2 Irradiation growth

Irradiation growth is a change in the dimensions of a zirconium alloy reactor component even though the applied stress is nominally zero. Irradiation growth is strongly affected by temperature, fast neutron fluence, Cold Work (CW) texture, and material chemistry (alloying and impurity elements)-recent results also suggest that hydrogen may impact irradiation growth rate.

Irradiation growth data is given in (Figure 3-6) with growth in sponge S-E110 material in green and electrolytic e-E110 in red. It is seen that e-E110 has higher growth and earlier breakaway than S-E110. For comparison purposes data for M5 (always from sponge) [Mardon et al 2005], and for an older version of e-E110 [Shishov et al 2005] have been added to the plot. The first point of interest is the difference between the "old'E110 (black ovals) and the newer e-E110, which supposedly are both made from the standard electrolytic/iodide Zr source. The difference is due to that the "old" E110 samples were contaminated with hydrogen during the irradiation in the test reactor Research Fast Reactor (BOR)60. Later investigations have shown that hydrogen may accelerate irradiation growth rate. In the recent data (e-E110 and S-E110), the samples were protected from hydriding of the Na coolant by a thin oxide film. Interestingly, M5 growth falls between the two Russian varieties.

The data compilation illustrates that there is a strong effect of Zr source, probably through the effects of minor impurities. No chemical composition information is given by Novikov, et al., but it is indicated orally that the main differences between e-E110 and S-E110 were Fe (100 vs. 300 ppm), Si (50-100 vs. <20 ppm) and O (200 vs. 500-600 ppm). For comparison purposes, M5 has about 500 ppm Fe, <20 ppm Si, 1400 ppm O and 25 ppm S. *The interested reader is referred to Section 6 in ZIRAT11/IZNA6 AR, 2006 for more information about this topic.*

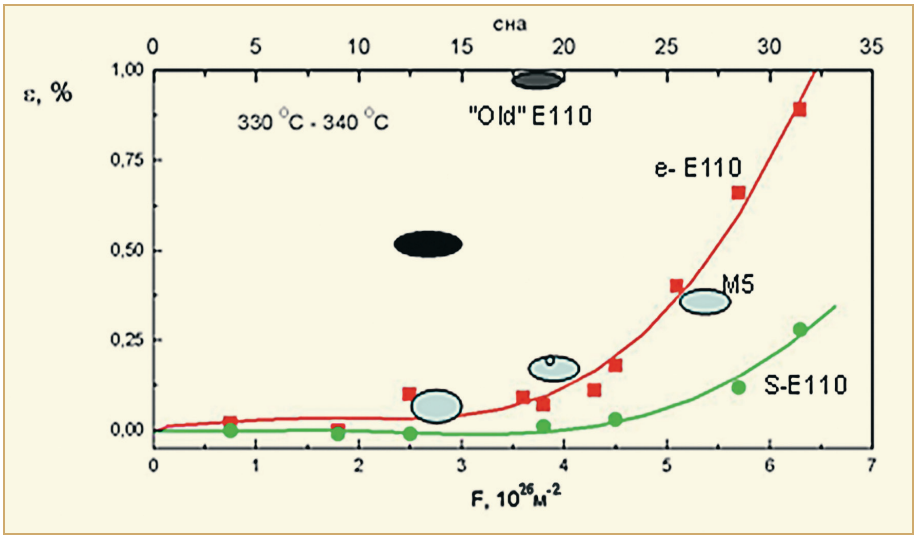

Figure 3-6: Irradiation growth of Zr1Nb alloys as a function of fluence, n/m^2 >0.1 MeV, at about 330 °C (613 K). Original data points for electrolytic/Zr iodide e-E110 (red) and sponge S-E-110 (green), [Novikov et al 2006]. Data added for M5 (blue), [Mardon et al 2005] and old E110 (black), [Shishov et al 2005]. To convert data to n/m^2 E>1 MeV in a PWR must divide fluence by a factor of 3.3, [Shishov et al 2005].

Irradiation growth will change the dimensions of FA components, specifically increase the length of the tubular product (irradiation growth will change dimensions also for flat products, such as e.g. fuel channels and Zr alloy grids/spacers – however, these components are not treated in this STR). Other processes which will change FA components are:

- *Creep (provided the component is subjected to stresses) including residual stress relaxation.*
- *Hydriding*

Below are some examples of potential issues related to dimensional changes of tubular products where irradiation growth contributes:

- *Excessive fuel rod length increase may lead to fuel rod bowing, potentially causing:*
  - *Rod-rod fretting failures.*
  - *Decrease in thermal margins Departure from Nucleate Boiling ((DNB)/dryout).*
- *Excessive guide tube growth leading to FA bowing, and twisting (PWRs) resulting in:*
  - *Decrease in thermal margins (DNB, LOCA) and increased fuel rod corrosion.*
  - *Difficulties in the insert of control rods.*
  - *Handling problems (leading to e.g. grid damages).*

More information about Irradiation growth may be obtained in the following ZIRAT/IZNA STRs:

- *ZIRAT10/IZNA5 STR on Impact of Irradiation on Material Performance, [Adamson & Cox 2005/2006].*
- *ZIRAT7/IZNA2 STR on Dimensional Stability of Zirconium Alloys, [Adamson & Rudling 2002/2003].*

3.3 Ingot melting process

3.3.1 Process

This is the first stage where zirconium appears as an alloy. The scrap has already been recycled. The chemical composition will not be changed significantly by further fabrication steps, except for a possible gas (H,O,N) uptake. An outline of the ingot manufacturing process is shown in (Figure 3-7).

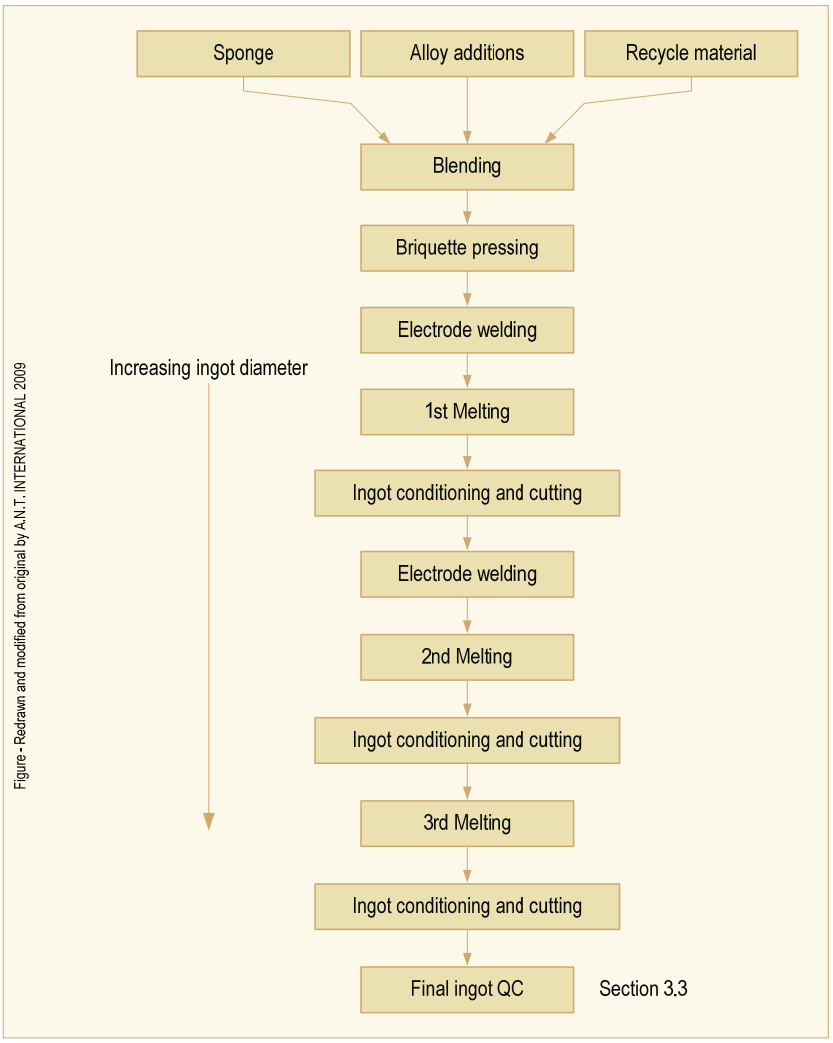

Figure 3-7: General process flow diagram for ingot fabrication. The section number relates to sections in this report where more information is given for each manufacturing step.

Briquettes of zirconium sponge recycle material from earlier manufacturing, and alloying elements blended with sponge are put together into an electrode in a specific sequence distributed along the length of the electrode. The alloying elements are added as compounds with melting temperatures similar to that of zirconium for homogeneity purposes. Normally, sponge-based briquettes containing the alloying compounds and solid recycle material are assembled and welded either by Electron Beam (EB) in vacuum or plasma arc welding in argon atmosphere into an ingot, (Figure 3-8).

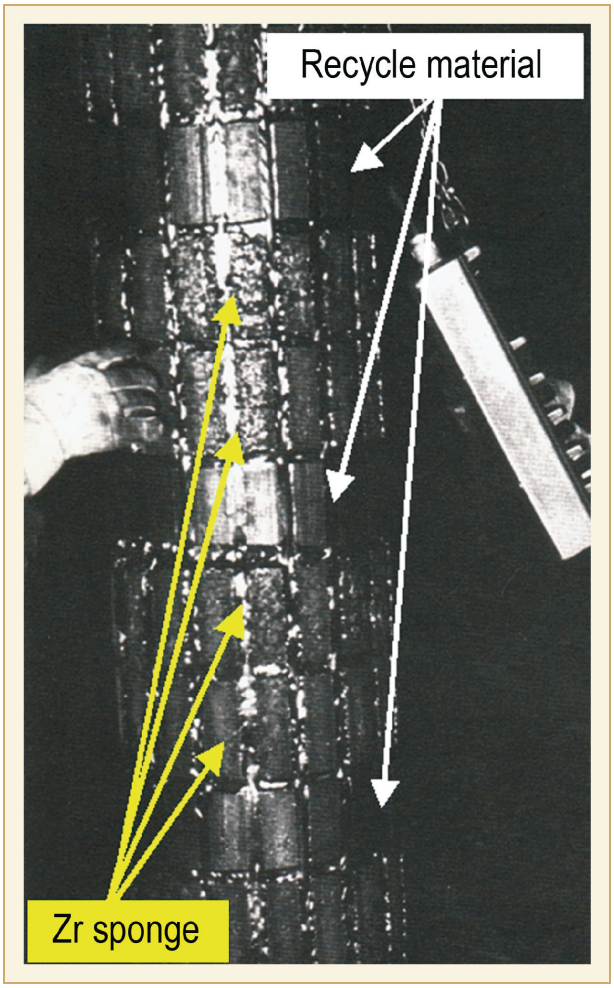

Figure 3-8: Consumable electrode showing sponge compacts and solid recycle sections. Original modified according to [Schemel 1989].

The subsequent melting is then normally done in vacuum to prevent oxygen and nitrogen pickup from the air. The consumable electrode is melted into a water-cooled copper mold slightly larger than the ingot diameter, (Figure 3-9). As the arc melts the metal, a fraction is solidified and forms a solid layer of the zirconium alloy in between the mold and the molten metal. Only a small fraction of the whole ingot is molten at any time during the continuous consumption of the electrode. Larger molten pool depth and volume increases homogeneity of the solidified ingot since diffusion and convection will take place during longer time before the melt has solidified. Larger amperage results in a large pool size. If the cooling of the mold is not done properly, copper may contaminate the ingot.

To increase the size and homogeneity of the ingot, the zirconium alloy electrode is melted three or four times. After each melting, the resulting ingot is cut up in cylindrical pieces which are assembled and welded (EB welding in vacuum) in a different sequence compared to that of the previous electrode.

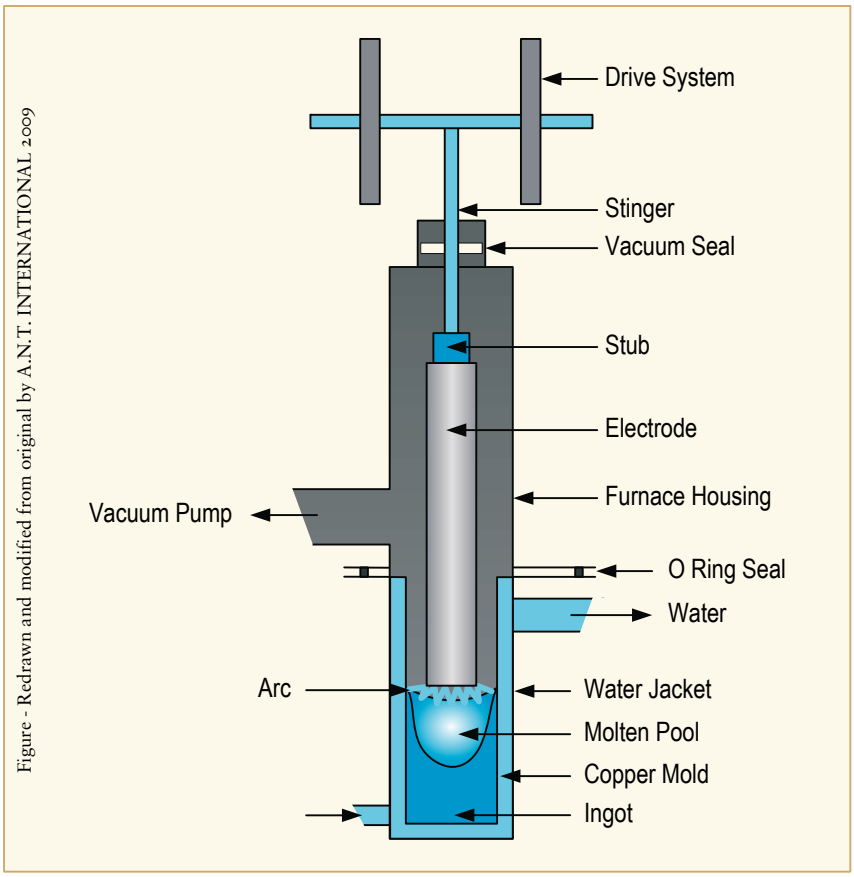

Figure 3-9: Schematics showing consumable vacuum arc melting.

3.3.2 Impact of ingot melting on material microstructure and in-pile performance

3.3.2.1 General

Process parameters that influence the characteristics and quality of the ingot are:

1) Quality of the raw material.

2) Molten pool diameter and depth which are functions of amperage and speed of melting.

3) Number or remelts of the ingot, - an increased number of remelts tends to increase the homogeneity in the material. Most manufacturers are using three remelts (triple melting).

4) Sequence of order of cut up cylindrical pieces from ingot from previous melting also impacts ingot homogeneity. Ingot alloying element inhomogenieties within an ingot result in variation in properties of the final products.

5) Electrode welding and copper mould atmosphere composition.

3.3.2.1.1 Microstructure

The alloying elements and impurities of modern zirconium alloys, such as Sn, Nb, Fe, Cr, Ni, O, Si, C are either fully dissolved in the alloy matrix (Sn, O) or dissolved to a large extent (Nb) or almost fully precipitated in small intermetallic second phase particles (Fe, Cr, Ni, Si, C), Second Phase Particle (SPPs).

The alloying elements in solid solution may impact the corrosion and hydriding properties as well as strength of the material, while the SPPs mainly affect the corrosion and hydriding performance.

In the majority of cases, impurities will degrade the properties and characteristics of materials. Therefore, their contents are restricted by the standards and specifications for zirconium, its alloys and the resulting FA structural parts.

The basis for these restrictions is the requirements to preserve low neutron capture, high corrosion resistance, processability and crack resistance during manufacturing as well as reliable operation in reactors. Among the impurities that are most important in this respect are C, N, Al, H, Cl, P, Hf, F, as follows:

- N, Al and C impurities are most harmful for corrosion of zirconium.
- C, H, Si, Cl, P and F impurities decrease the ductility of zirconium and its alloys, thus, degrading processability and crack resistance.
- Cd, B, Hf and Co are elements that increase the neutron capture.
- O increases strength and affects corrosion and ductility to some degree.
- Fe and Cr favourably influence the corrosion of zirconium, for this reason their allowable contents are much higher.

The typical requirements specified for impurity contents of zirconium and its alloys are summarized in (Table 3-3).

Table 3-3: ASTM Standard B353 for Zr and its alloys used in nuclear industry (content of impurities).

Element	Pure Zr	Zry-2	Zry-4	Zr-Nb (2.4-2.8%Nb)	Zr-Nb (2.5-2.8%Nb)
Impurity, max (ppm)					
Al	75	75	75	75	75
B	0.5	0.5	0.5	0.5	0.5
Cd	0.5	0.5	0.5	0.5	0.5
C	270	270	270	270	150
Cr	200	-	-	200	200
Co	20	20	20	20	20
Cu	50	50	50	50	50
Hf	100	100	100	100	100
H	25	25	25	25	25
Fe	1500	-	-	1500	650
Mg	20	20	20	20	20
Mn	50	50	50	50	50
Mo	50	50	50	50	50
Ni	70	-	70	70	35
N	80	80	80	80	65
Pb	-	-	-	-	50
Si	120	120	120	120	120
Sn	50	-	-	50	100
Ta	-	-	-	-	100
Ti	50	50	50	50	50
U	3.5	3.5	3.5	3.5	3.5
V	-	-	-	-	50
W	100	100	100	100	100

The different types of SPPs which can appear in Zr alloys are summarised in (Table 3-4) and described more in the following.

In Zr-Fe alloys, the orthorhombic Zr_3Fe phase appears whereas in Zr-Cr alloys the hexagonal Laves phase $ZrCr_2$ exists. In zirconium alloys that contain Fe and Cr, such as Zircaloy-4, the type of SPP depends on the Fe/Cr ratio. If the Fe/Cr alloying ratio is <4, the only phase formed is the Laves phase, $Zr(Cr,Fe)_2$. At a Fe/Cr alloying ratio of >4 Zr_3Fe or Zr2, Fe is also formed. The size of the Laves phase precipitates is smaller than the size of the Zr_2Fe precipitates and the Zr_3Fe precipitates are generally significantly larger than the other two precipitate types. One of the most important zirconium alloys, Zircaloy-2, contains Ni in addition to Sn, Fe and Cr. In this system, two different types of SPP are formed. These are the hexagonal Laves phase, $Zr(FeCr)_2$, and the body-centred tetragonal Zintel phase, $Zr_2(FeNi)$. The size of the Zintel phase precipitates is somewhat larger than that of the Laves phase precipitates.

Zr-Nb alloys usually contain fine precipitates of β-Nb (80%Nb20%Zr) or β-Zr (20%Nb80%Zr) depending on fabrication route. Several modern Zr-Sn-Nb alloys, such as ZIRLO or E635, contain about 1 wt% Nb as well as 0.1 to 0.5 wt% Fe. Furthermore, most binary Zr-Nb alloys, such as M5 or Zr-2.5Nb, contain some Fe as an impurity (several 100 ppm by weight). At high Nb and moderate Fe concentrations, a hexagonal $Zr(NbFe)_2$ phase, with Nb/Fe=1-1.5, is often found besides the fine β-Nb precipitates. At medium Fe and not too high Nb contents all SPPs are of the Laves phase $Zr(NbFe)_2$ type. At high Fe and rather lower Nb concentrations a cubic $(ZrNb)_2Fe$ phase may be formed in addition to the Laves phase or even replacing the Laves phase. The size of the $Zr(NbFe)_2$ precipitates in fully α-processed Zr-Nb alloys with some iron is, even in low-temperature-processed material, quite large (100-200 nm) and larger than the size of the β-Nb precipitates (~50 nm). The $(ZrNb)_2Fe$ phase is the largest (500 nm).

C or Si impurities form binary SPPs with zirconium only during processing in the β-range if their content is above 150 and 50 ppm, respectively. In the α-Zr range, Si and Fe usually form the body centered tetragonal (bct) $Zr_2(FeSi)$ phase. The size of the $Zr_2(FeSi)$ phase is generally very small and much finer than that of the usual Laves SPP in Zircaloy-4.

Hydrides usually precipitate as platelets closely parallel to the c- plane of the hexagonal crystal structure inside the grains or on the grain boundaries.

Table 3-4: Type and characteristics of SPP in zirconium alloys. Information from [Adamson et al 2002/2003].

Alloying elements	Solubility in α (%)	Trans. Temp. α/ (α+β) (°C)	Type of SPP	Structure of SPP	Max existing temp. (°C)	Size (μm)/distribution after processing in		
						low α range	high α range	(α+β) range
Fe	0.01	795	Zr_3Fe or Zr_2Fe	Orthorhombic bct	885 998	0.5/uniform	1/uniform	
Cr	0.01	830	$ZrCr_2$	Laves, fcc	1560	0.02/uniform	0.15/uniform	
Fe+Cr	0.01	800	$Zr(Fe,Cr)_2$	Laves, usually hex.		0.04/uniform	0.2/uniform	0.4/at GB*
Fe+Ni	0.01	800	$Zr_2(Fe,Ni)$	Zintel, tetrag		0.2/uniform	0.7/uniform	
Nb	0.5	620	β-Nb or β-Zr	bcc	2000 1740	0.03/uniform	0.05/uniform	>0.1/at GB*
Nb+Fe	0.3/0.01	600	$Zr(Fe,Nb)_2$ or $(Zr,Nb)_2Fe$	Laves, hex tetrag/fcc	~700 ~750		0.15/uniform 0.5/uniform	0.7/at GB*
Nb+Fe+Cr	0.3/0.01	600	$Zr(Fe,Cr,Nb)_2$	Laves, hex			0.15/uniform	
Impurities								
C	3	800	ZrC		3427			at>150 ppm >0.1 μm
Si	0.01	860	Zr_3Si		1650		0.05/uniform	at>150 ppm >0.1 μm
Si+Fe	0.01	800	$Zr_2(Fe,Si)$					
H	0.06	550	Zr_2H					

* Grain Boundaries

ZrNbFe Alloys - The SPPs that form in ZrNbFe alloys with different compositions upon β-quenching and subsequent processing in the α-range, at temperatures below 600 °C, are shown in (Figure 3-10). This figure also shows the types of SPPs formed in different Zr-Nb-Fe alloys. The Sn content in Zr-Nb-Fe alloys plays only a very minor role in the type of SPP formed. Sn is usually fully dissolved in the matrix.

If the Fe (Transition Metal (TrM)) content is low (<100 ppm), only very small (50 nm) β-Nb precipitates, containing 85-90%Nb, exist in the matrix. The number density of these β-Nb SPP increases with increasing Nb alloying content.

If Fe is added to the ZrNb alloy, medium-large $Zr(NbFe)_2$ SPP (Laves phase) are also formed (100-200 nm), containing about 40wt%Zr, 40wt%Nb and 20wt%Fe. With increasing Fe content, the fraction of β-Nb SPPs decreases while the fraction of $Zr(NbFe)_2$ SPPs increases. At a certain Fe/Nb alloying ratio, Fe ≥0.44·(Nb-0.4)[23] β-Nb SPP are no longer formed.

Increasing the Fe/Nb alloying ratio further at an Fe ≥1.6·(Nb-0.3) gives large $(ZrNb)_2Fe$ SPPs (300-1000 nm) with about 65%wtZr, 15%wt%Nb and 20wt%Fe. At a higher Fe/Nb alloying ratio, large Zr_3Fe SPPs are also formed. At very low Nb contents (<0.3%) the large Zr_3Fe SPPs are the only precipitates in the matrix.

If Cr or V is added at a concentration of >0.25·Fe, either $Zr(NbCr)_2$ or $Zr(NbV)_2$ (Laves phase) SPP are stabilized. This stabilization takes place even at low (<0.3%) Nb contents.

After long annealing times in the upper α-Zr temperature range only 0.3-0.5% Nb and a very low content of TrMs (some100 ppb) remain in the α -Zr matrix, [Toffolon et al 2001] and [Shishov et al 2005]. The Nb solubility in α-Zr at 580 °C decreases from 0.5% to 0.3% by Fe additions of >100 ppm.

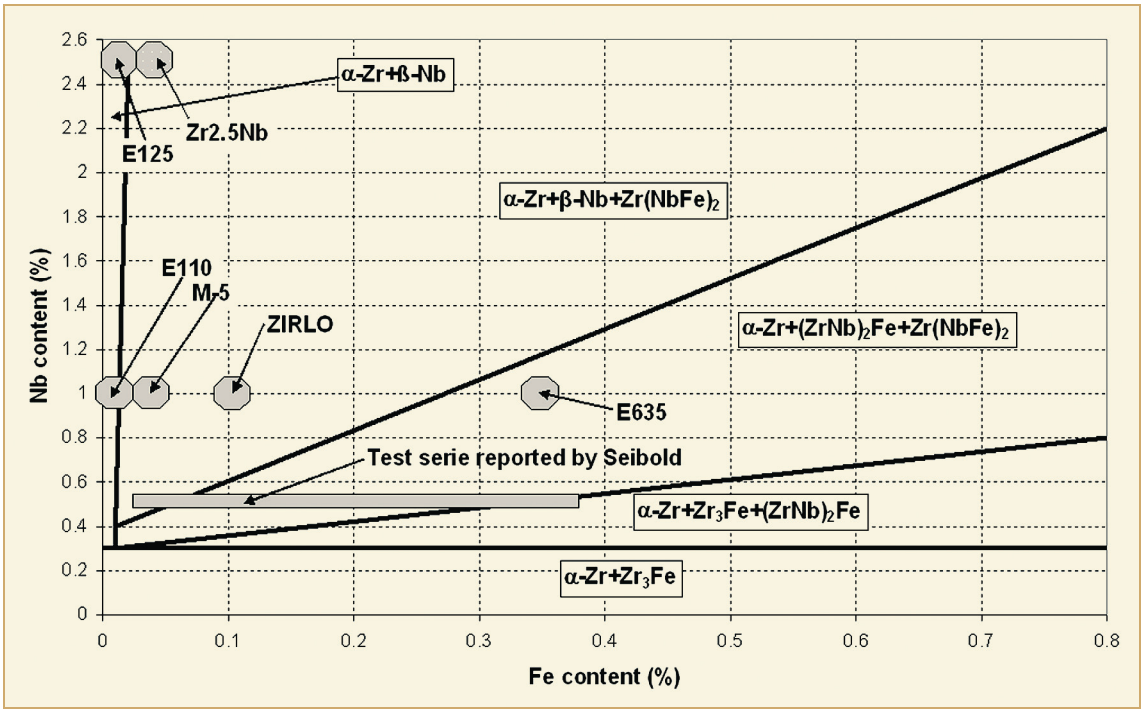

Figure 3-10: Zr-Nb-Fe ternary alloy phase diagram composed from information in [Toffolon et al 2002] and [Shishov et al 2005].

[23] This mean Fe greater than or equal to 0.44x(Nb – 0.4)

In-reactor dissolution of SPPs - At normal Light Water Reactor (LWR) temperatures (270-370 °C (543-643 K)) the SPPs change under irradiation in a combination of two ways – amorphization and dissolution.

Amorphization means that the original SPP crystalline structure is converted to an amorphous structure. A critical temperature exists above which the annealing processes are fast enough to prevent the accumulation of defects needed to transform crystalline SPPs to amorphous structures. For low temperature irradiations, amorphization of both $Zr(FeCr)_2$ and $Zr_2(Fe,Ni)$ in Zry-2 occurs readily at temperatures near 100 °C (373 K). For the temperatures (300 °C (573 K)) and neutron flux encountered in a LWR, $Zr(Fe,Cr)_2$ becomes amorphous but $Zr_2(Fe,Ni)$ does not. Above about 330 °C (603 K), neither type of SPP becomes amorphous.

The fluence required to produce complete amorphization depends on neutron flux, temperature and SPP size and chemistry. But, for typical $Zr(Fe,Cr)_2$ SPPs of initial size near 0.1 μm, the entire SPP is amorphous by end of bundle life burnups, <50 MWd/KgU ($1x10^{26}$ n/m^2, E>1 MeV). *The rate of dissolution depends on the SPP size, with higher rates for smaller sizes. The extent of dissolution depends on size and fluence.* It has been demonstrated in a BWR that small (<0.04 μm) SPPs in Zry-2 can completely dissolve at low to moderate burnups. Also in a PWR at temperatures near 290 °C, SPPs in Zry-4 with an average size of 0.2 μm were >80% dissolved at moderate burnup (1×10^{26} n/m^2, E > 1MeV). ***The consequence of the complete dissolution of the SPPs in Zry-2 and Zry-4 is a dramatic increase in the Hydrogen PickUp Fraction (HPUF) and, after some time, also an acceleration of the corrosion rate in BWRs.*** It must be noted, however, that nodular corrosion in BWRs can be adversely affected by the presence of large SPPs at the outer cladding surface and that cladding performance depends on the composition and size of the precipitates across the wall thickness.

For the Zr-Nb type alloys preferentially used in PWRs neither the βNb nor Zr $(Nb, Fe)_2$ SPPs become amorphous (or dissolve) for irradiation temperature >330 °C (603 K).

SPP amorphization in itself does not appear to affect material behaviour; however, dissolution of both amorphous and crystalline SPPs does influence corrosion and growth.

3.3.2.1.2 Performance

Corrosion and hydrogen pickup - The effect of a specific alloying element on the corrosion rate depends on both the cladding chemistry and on the operating environment, as can be seen from (Table 3-5) and (Table 3-6), as follows:

- Sn increases the rate of uniform corrosion in hydrogenated environments and reduces the time to transition but decreases nodular corrosion in a BWR. Sn also decreases the rate of corrosion in a PWR with diluted LiOH.

- Nb is very beneficial for uniform corrosion resistance if no Fe, Cr, Ni, V are added. However, Nb-containing alloys can suffer from increased rates of corrosion under oxygenated coolant conditions, e.g. in BWRs. Nb reduces corrosion rates in hydrogenated water and steam in the concentration range up to 0.5%, where Nb is in solid solution in the α-Zr matrix. The Nb will end up homogeneously distributed in the zirconium oxide.

- The transition elements (TrM) Fe, Cr, Ni, V, Cu reduce uniform corrosion rate in Nb-free alloys out of pile, in PWRs and in LiOH-containing water. Contrary to Nb, the TrM alloying elements Fe, Cr, Ni, V, and Cu, which all have a very low solubility in the α-Zr, induce the lowest corrosion rate at concentrations far above their solubility limit in the α-Zr matrix. Thus, corrosion of Zr-TrM alloys is governed by the intermetallics (SPP) and the beneficial effect of the SPPs arising from local spots of high TrM concentration within the oxide.

- Zr-Sn-TrM alloys with a low TrM content usually show a significant corrosion acceleration at longer exposure times, whereas higher TrM contents reduce this late corrosion acceleration, [Broy et al 2000]. In this respect, Fe and Ni are more beneficial than Cr, V, and Cu, at least in PWRs and out of pile. Cr and V can, under certain conditions, increase corrosion out of pile and in PWRs. In BWRs, the effect of transition elements on corrosion rate is not so clear. Irradiation of Zircaloy-2 and -4 in BWRs can increase the corrosion rate significantly, particularly, if the material has fine SPPs that dissolve to a large extent under irradiation, [Cheng et al 1994].
- Nitrogen in solid solution in the concentration range of >30 to 120 ppm, increases corrosion rate significantly (depending on the alloy composition).
- Oxygen, which is also soluble in the studied range, increases corrosion slightly.
- Carbon increases corrosion at concentrations above about 100 ppm, when it precipitates as carbides.
- Si, in the range of 80 and 120 ppm, can reduce the corrosion rate if the β-quenching step during the alloy manufacturing was not perfect. Fine silicides can act as nucleation sites for Zr-FeCrNi SPPs, making the SPP distribution more homogeneous thereby reducing corrosion rate for lots not subjected to fast Beta Quenching (BQ). At higher concentrations of Si (>150 ppm) the corrosion rate is increased and probably the hydrogen pick-up fraction is decreased.
- P increases nodular corrosion rate at >10 ppm but has no effect on uniform corrosion rate in the studied range.
- Mn increases corrosion rate if it exceeds the solubility limit in α-Zr.
- Al, which is fully soluble in α-Zr, increases corrosion rate if the content is above 80 ppm.
- S has no effect on the uniform corrosion rate in the studied range.

Table 3-5: Effect of alloying elements on zirconium alloy corrosion rate. "HPUF" =Hydrogen PickUp Fraction, [Adamson et al 2007/2008a].

Element	Solubil. (%)	Best alloy content[24] (%)	Out-pile corrosion	In-PWR corr.	LiOH corr.	In-BWR corr.	HPUF
Sn	2	0/>1	—	=	+ +	+	0
Nb	0.5	0.5/>2	+ +	+ +	0	—/+	+/**0**
Fe	<0.01	≥0.3	+ +	+ +	+ +	+	0/+
Cr	<0.01	≥0.15	+/—	+	+ +	+	+ (>0.15)
Ni	<0.01	0.05	+ +	+		+	=/0
V	<0.01	≥0.15	+/—	+	+ +	+	+
Cu	<0.1	≥0. 5	+				0

0: no effect, — increase, = strong increase, + reduction, ++ strong reduction, 0/+ effect differs in different environments.

[24] To get best corrosion and hydriding performance.

Table 3-6: Effect of impurities on zirconium alloy corrosion rate, [Adamson et al 2007/2008a].

Element	Conc. studied (ppm)	Out-pile	In-PWR	In-BWR
O	600-2000	—/0	0	—
N	20-2000	=	=	=
Si	<120/>120-	+/—	+	+
C	<100/>100-300	0/—	—	0
Al	<80/>80-400	0/—		
Mn	<300/>300-5000	0/—		
P	3-25	0		—
S	1-40	0		

0: no effect, — increase, = strong increase, + reduction, ++ strong reduction, 0/+ sometimes

(Figure 3-11) show early results of the impact of impurities and alloying elements on hydrogen uptake in out-of-reactor autoclave tests.

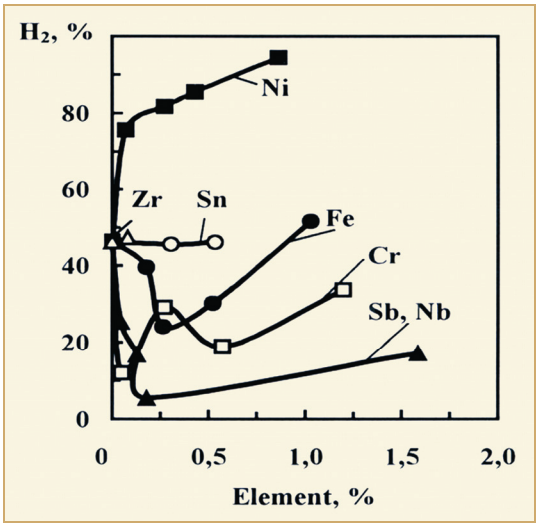

Figure 3-11: HPUF during out-of-reactor zirconium corrosion in 350 °C water as a function of alloying elements, [Amaev et al 1964].

The size, distribution and kind of SPP can play a significant role in out-of-pile corrosion in oxygen-free water and steam, in PWRs/VVERs and in BWRs. However, the effect is different for different alloys, as can be seen from (Table 3-7).

Table 3-7: Effect of SPP size on corrosion of zirconium alloys.

Alloy type	Effect of SPP size on corrosion in			
	350 °C water	500 °C steam	In-PWR	In-BWR
Zr-Sn-Fe, Cr	Increases <70 nm	Increases <150 nm	Increases < 80 nm	Increases <80 nm and at >150 nm
Zr-Nb-Sn	Slightly lower at very fine size	Slightly lower at very fine size	Significantly lower at very fine size	Slightly lower at very fine size
Zr-Nb-(Sn)-Fe,Cr	Slightly lower at very fine size	Slightly lower at very fine size	Significantly lower at very fine size	Slightly lower at very fine size

However, it has to be mentioned that it is not fully clear whether these effects are primarily due the SPP characteristics or due to the solute content. Some scientists consider the solute content of Fe and Cr as the real root cause for the observed differences, e.g. [Cheng & Adamson 1987]. The α-Zr solute content increases with decreasing SPP size and annealing (A)-parameter. The solute content can affect the stoichiometric structure of the zirconium oxide layer, by replacing Zr^{+4} by subvalent atoms, such as Fe^{+3}, Cr^{+3}, Ni^{+2}…, thereby increasing the oxygen vacancy concentration and affecting the oxide electrical conductivity. Fine SPPs with a high surface energy are in equilibrium with an increased solute content. Furthermore, fine SPPs dissolve after rather low neutron fluences in BWRs. The often-observed late-accelerated corrosion in BWRs, that starts earlier the finer the SPPs are, might well be initiated by the super-saturation of the transition elements in α-Zr metal. Ex-reactor corrosion tests on irradiated material have shown increased corrosion rates, which depend upon fast fluence and initial SPP size, [Cheng et al 1994]. However, the observed increased out-of-pile or in-PWR corrosion rate of Zircaloy-4 with a low A-parameter (SPP size) does not require an irradiation-induced dissolution of the SPP. It arises if the SPP size is below a threshold value which depends on a particular exposure time.

In-BWRs, an increase in hydrogen pick-up is observed before the onset of increased corrosion rate, at least in Zircaloy-2.

Improved corrosion resistance of zirconium alloys in water can be either achieved by the addition of >0.3 % Fe+Cr+Ni, which primarily is located in SPPs, or by an Nb content of ≥0.3%. Nb is distributed in the metal uniformly as a solute up to a concentration of 0.3-0.5%. Only at higher concentrations do β-Nb or Zr-Nb-Fe, Cr SPPs arise in such alloys. Obviously, in alloys which have a good corrosion resistance due to sufficient Nb solute content, SPPs do not play an important role, whereas in alloys which have good corrosion resistance, primarily due to Fe, Cr, Ni, and V present in SPPs, an optimum SPP size is needed.

The interested reader of the impact on alloying/impurities on Zr alloy corrosion and hydrogen pickup performance is referred to e.g. Section 3 and 4 authored by Friedrich Garzarolli in ZIRAT12 STR on "Corrosion Mechanisms in Zirconium Alloys", 2007.

4 References

Abe H., Takeda K., Uehira A., Anada H. and Furugen M., "*A new fabrication process for Zr-lined Zry-2 tubing*", Zirconium in the nuclear industry, Twelfth international symposium, ASTM STP 1354, G. P. Sabol and G. D. Moan, EDS., American Society for Testing and Materials, pp. 425-459, West Conshohocken, PA, 2000.

Abriata J. P. and Bolcich J. C., Bull. Alloy phase diagrams, V. 3, N1, pp. 34, 1982.

Abriata J. P., Artas D. and Bolcich J. C., Bull. Alloy diagrams, V. 4, N2, pp. 147-154, 1983.

Abriata J. P., Garces J. and Versaci R., Bull. Alloy phase diagrams, V. 7, N2, pp. 116-124, 1986.

Adamson R. B. and Rudling P., "*Mechanical Properties of Zirconium Alloys*", ZIRAT6/IZNA1 Special Topics Report, ANT International, Skultuna, Sweden, 2001/2002.

Adamson R. B. and Rudling P., "*Dimensional Stability of Zirconium Alloys*", ZIRAT7/IZNA2 Special Topics Report, ANT International, Skultuna, Sweden, ANT International, 2002/2003.

Adamson R. B., Cox B., Garzarolli F., Strasser A., Rudling P. and Wikmark G., "*Corrosion of Zirconium Alloys*", ZIRAT7/IZNA2 Special Topics Report, ANT International, Skultuna, Sweden, 2002/2003.

Adamson R., Cox B., Garzarolli F., Strasser A. and Rudling P., "*ZIRAT9/IZNA4 Annual Report*", ANT International, Skultuna, Sweden, 2004/2005.

Adamson and Cox, "*Impact of Irradiation on Material Performance*", ZIRAT10/IZNA5 Special Topics Report, ANT International, Skultuna, Sweden, 2005/2006.

Adamson R., Cox B., Davies J., Garzarolli F., Rudling P. and Vaidyanathan S., "*Pellet-Cladding Interaction (PCI and PCMI)*", ZIRAT11/IZNA6, Special Topics Report, ANT International, Skultuna, Sweden, 2006/2007a.

Adamson R. B., Cox B., Garzarolli F., Riess R., Sabol G., Strasser A. and Rudling P., "*ZIRAT11/IZNA6 Annual Report*", ANT International, Skultuna, Sweden, 2006/2007b.

Adamson R., Garzarolli F., Cox B., Strasser A. and Rudling P., "*Corrosion Mechanisms in Zirconium Alloys*", ZIRAT12/IZNA7 Special Topics Report, ANT International, Skultuna, Sweden, 2007/2008a.

Adamson R., Cox B., Garzarolli F., Sabol G. Strasser A. and Rudling P., "*ZIRAT12/IZNA7 Annual Report*", ANT International, Skultuna, Sweden, 2007/2008b.

Amaev A. D., Ambartsumyan R. S., Kiselev A. A., Konobeevskiy S. T., Anisomova J. A., Glukhov A. M., Lebedev L. M., Myshkin V. A., Goncharov V. V., Ivanov E. G., Orlov M. S., Pravdyuk P. F., Ryazantsev E. P. and Skvortsov V. V., "*Influence of some factors upon hydriding and variation properties of zirconium alloy with 1%Nb used for fuel element cladding in water-moderated water-cooled power reactors*", Proc. 3rd U.N. Int. Conf. on Peaceful Uses of Atomic Energy, Geneva, CH, A/Conf.28/P/342, 1964.

Andersson T., et al., "*Influence of thermal processing and microstructure on the corrosion behaviour of Zircaloy-4 tubing*", IAEA SM 288/59, IAEA, Vienna, 1986.

Aomi M. et al., "*Evaluation of Hydride Reorientation Behavior and Mechanical Property for High Burnup Fuel Cladding Tube in Interim Dry Storage*", Zr in the Nuclear Industry, 15th International Symposium, Sunriver (OR), June 25th-28th, 2007.

Arias D. and Abriata J. P., Bull. Alloy phase diagrams, V. 9, N5, pp. 597-604, 1988.

Bai J. Gilbon J., Prioul C. and Francois D., "*Hydride Embrittlement in Zircaloy-4 Plate, Part I Influence of Microstructure on the Hydride Embrittlement in Zircaloy-4 at 20°C and 350°C" and "Part II, Interaction Between the Tensile Stress and the Hydride Morphology*", Met. and Materials Transactions, v. 25A, June, 1994.

Bangaru N. V., Busch R. A. and Schemel J. H., "*Effect of beta-quenching on the microstructure and corrosion of Zircaloys*", Zirconium in the nuclear industry, Seventh international symposium, ASTM STP 939, R. B. Adamson and L. F. P. Van Swam, Eds., American Society for Testing and Materials, pp. 341-363, Philadelphia, 1987.

Bement A. L., Tobin J. C. and Hoagland R. G., "*Effects of Neutron Irradiation on the Flow and Fracture Behavior of Zircaloy-2*", Flow and Fracture, *ASTM*-STP 380, *ASTM*, 364-383, 1965.

Besch O. A., Yagnik S. Y., Woods K. N., Eucken C. M. and Bradley E. R., "*Corrosion behaviour of duplex and reference cladding in NPP Grohnde*", Zirconium in the Nuclear Industry: Eleventh International Symposium", ASTM STP 1295, Bradley E. R. and Sabol G. P., Eds. American Society for Testing and Materials, pp. 805-824, West Conshohocken, 1996.

Billone M., Yan Y. and Burtseva T., "*ANL Research Results Relevant to LOCA Embrittlement Criteria", Parts 1, 2 and 3*. ACRS Reactor Fuels Subcommittee Meeting, NRC, Rockville MD, January 19, 2007.

Bossis P., Verhaeghe B., Doriot S., Gilbon D., Chabretou V., Dalmais A., Mardon J.P., Blat M. and Miquet A., "*In PWR Comprehensive Study of High Burn-up Corrosion and Growth Behavior of M5 and Recrystallized Low-Tin Zircaloy-4*", 15th ASTM International Symposium: Zirconium in the Nuclear Industry – Sun River, OR, June 20, 2007.

Broy Y., Garzarolli F., Seibold A. and Van Swam L. F., "*Influence of Transition Elements Fe, Cr, and V on Long-Time Corrosion in PWRs*", Zirconium in the Nuclear Industry: 12th Int'l Symposium, *ASTM* STP 1354, G. P. Sabol and G. D. Moan, Eds., *ASTM*, West Conshohocken, PA, 609-622, 2000.

Causey A. R., Fidleris V., MacEwen S. R. and Schulte C. W., "*In-reactor deformation of Zr2.5Nb pressure tubes*", ASTM Spec. Techn. Publ. 956, pp. 54-, 1988.

Chang K. I. and Hong S. I., "*Effect of Sulfur on the Strengthening of a Zr-Nb Alloy*", Journal of Nuclear Materials, 373, pp. 16-21, 2008.

Charquet D. and Alheritiere E., "*Influence of Impurities and Temperature on the microstructure of ircaloy-4 and Zircaloy-2 after the beta-alpha phase transformation*", ASTM STP 939, pp. 284-291, 1987a.

Charquet D., Steinberg E. and Millet Y., "I*nfluence of Variations in Early Fabrications Steps on Corrosion, Mechanical Properties, and Structure of Zircaloy-4 Products*", Zirconium in the Nuclear Industry: 7th Int'l Symposium, ASTM STP 939, Adamson R. B. and Van Swam L. F. P., Eds., ASTM, Philadelphia, 431-447, 1987b.

Charquet D., Hahn R., Ortlieb E., Gros J. P., Wadier J. F., 8th International Conference on Zirconium in Nuclear Industry, ASTM STP 1023, L. F. P. Van Swam and C. E. Eucken, Eds., American Society for Testing and Materials, pp. 405-422, Philadelphia, PA, 1989.

Charquet, D., Senevat, J., Mardon, J., "*Influence of Sulfur Content on the Thermal Creep of Zirconium Alloy Tubes at 400°C*", Journal of Nuclear Materials, 255, pp. 78-82, 1998.

Charquet D., "*Microstructure and properties of zirconium alloys in the absence of irradiation*", Zirconium in the nuclear industry, Twelfth international symposium, ASTM STP 1354, G. P. Sabol and G. D. Moan, EDS., American Society for Testing and Materials, pp. 3-14, West Conshohocken, PA, 2000.

Cheadle B. A., Ells C. E. and van der Kuur, J., "*Plastic Instability in Irradiated Zr-Sn and Zr-Nb Alloys*", Zirconium in Nuclear Applications, *ASTM* STP 551, American Society for Testing and Materials, 370-384, 1974.

Cheadle, B. A. "*Fabrication of Zirconium Alloys into Components for Nuclear Reactors*", Zirconium in the Nuclear Industry, ASTM STP 633, A. L. Lowe, Jr. and G. W. Parry, Eds., American Society for Testing and Materials, 457-485, 1977.

Cheng B., Adamson R. B., Bell W .L. and Proebstle R. A., "*Corrosion performance of some Zr alloys irradiated in the Steam Generating Heavy Water Reactor, Winfrith*", Proc. 1st Conference on Environmental Degradation in Nuclear Power Systems, pp. 273-296, Myrtle Beach, 1983.

Cheng B. and Adamson R. B., "*Mechanistic Studies of Zircaloy Nodular Corrosion*", Zirconium in the Nuclear Industry: 7th Int'l Symposium, *ASTM* STP 393, Adamson R. B. and Van Swam L. F. P., Eds., *ASTM*, Philadelphia, 387-416, 1987.

Cheng B-C., Krüger R. M. and Adamson R. B., "*Corrosion Behaviour of Irradiated Zircaloy*", Proc. 10th Int. Symp. in the Nucl. Ind., *ASTM*-STP-1245, pp. 400-418, 1994.

Chernaeva T. N., Stukalov A. I. et al, "*Oxygen in Zirconium*", Kharkov, KhFTI, p.111, 1999.

Choubey R., Aldridge S. A., Theaker J. R., Cann C. D. and Coleman C. E., "*Effects of Extrusion-Billet Preheating on the Microstructure and Properties of Zr2.5Nb Pressure Tube Materials*", Proc. 11th Int. Symp. on Zr in the Nucl. Ind., (E. R. Bradley and G. P. Sabol, Eds) ASTM-STPP-1295, pp. 657-675., ASTM, 1996.

Chung H. M., "*Differences in Behaviour of Sn and Nb in Zirconium Metal and Zirconium Dioxide*", SEGFSM Topical Meeting on LOCA Issues Argonne National Laboratory, May 25-26, 2004.

Cox B. and Rudling P., "*Hydriding Mechanisms and Impact on Fuel Performance*", ZIRAT5, Special Topics Report, ANT International, Skultuna, Sweden, 2000.

Cox B., Garzarolli F., and, Rudling R., "*Corrosion of Zr-Nb Alloys*", ZIRAT9/IZNA4 Special Topics Report, ANT International, Skultuna, Sweden, 2004/2005.

Cox B., Garzarolli F., Strasser A. and Rudling P., "*Structural Behavior of Fuel and Fuel Channel Components*", ZIRAT10/IZNA5 Special Topics Report, ANT International, Skultuna, Sweden, 2005/2006.

Cox B., Garzarolli F., Adamson R., Rudling P. and Strasser A., "*Fuel Material Technology Report, Vol. I*", ANT International, Skultuna, Sweden, 2006.

Dahlbäck M., L. Hallstadius L, Limbäck M., Bunel, G., Moinard P., Andersson T., Askeljung P., Flygar J. and Karlsson M., "*The Effect of Beta Quenching in Final Dimension on the Irradiation Growth of Tubes and Channels*", Proc. 14th *ASTM* Symposium on Zirconium in the Nuclear Industry, Stockholm, 2004.

Dahlbäck M., Hallstadius L., Limbäck M., Vesterlund G., Andersson T., Witt P., Izquierdo J., Remartinez B., Ciaz M., Sacedon J. L., Alvarez A. –M., Engman U., Jakobsson R. and Massih A. R., "*The Effect of Liner Component Iron Content on Cladding Corrosion, Hydriding and PCI Resistance*", 14th International Symposium on Zirconium in the Nuclear Industry, ASTM STP 1467, P. Rudling and B. Kammenzind, Eds., American Society for Testing and Materials, Journal of ASTM International, Vol.2,No.8,Paper ID JA112444, Sept. 2005a.

Dahlbäck M, Limbäck M., Hallstadius L., Barberis P., Bunel G., Simonot C., Andersson T., Askeljung P., Flygare J., Lehtinen B. and Massih A. R., "*The effect of beta quenching in final dimension on the irradiation growth of tubes and channels*", Journal of ASTM International, 2, June 2005, paper JAI12337, 2005b.